Available online at www.sciencedirect.com
SCIENCE DIRECT
Pattern Recognition 39 (2006) 2065–2076
PATTERN RECOGNITION
THE JOURNAL OF THE PATTERN RECOGNITION SOCIETY
www.elsevier.com/locate/patcog

A novel approach to the fast computation of Zernike moments

Sun-Kyoo Hwang*, Whoi-Yul Kim

Division of Electrical and Computer Engineering, Hanyang University, Seongdong-gu, Seoul 133-791, Republic of Korea

Received 16 June 2005; received in revised form 20 February 2006; accepted 8 March 2006

Abstract

This paper presents a novel approach to the fast computation of Zernike moments from a digital image. Most existing fast methods for computing Zernike moments have focused on the reduction of the computational complexity of the Zernike 1-D radial polynomials by introducing their recurrence relations. Instead, in our proposed method, we focus on the reduction of the complexity of the computation of the 2-D Zernike basis functions. As Zernike basis functions have specific symmetry or anti-symmetry about the x-axis, the y-axis, the origin, and the straight line $y = x$, we can generate the Zernike basis functions by only computing one of their octants. As a result, the proposed method makes the computation time eight times faster than existing methods. The proposed method is applicable to the computation of an individual Zernike moment as well as a set of Zernike moments. In addition, when computing a series of Zernike moments, the proposed method can be used with one of the existing fast methods for computing Zernike radial polynomials. This paper also presents an accurate form of Zernike moments for a discrete image function. In the experiments, results show the accuracy of the form for computing discrete Zernike moments and confirm that the proposed method for the fast computation of Zernike moments is much more efficient than existing fast methods in most cases.

Keywords: Zernike moments; Fast method; Symmetry/anti-symmetry; Discrete Zernike moments

1. Introduction

Zernike moments, a type of moment function, are the mapping of an image onto a set of complex Zernike polynomials. As these Zernike polynomials are orthogonal to each other, Zernike moments can represent the properties of an image with no redundancy or overlap of information between the moments [1,2]. Due to these characteristics, Zernike moments have been utilized as feature sets in applications such as pattern recognition [1,3], content-based image retrieval [4], and other image analysis systems [5,6]. Unfortunately, due to the high complexity of the definition, it takes an excessive amount of time to compute Zernike moments. This fact makes them unsuitable for real-time applications.

Several methods to speed up the computation of Zernike moments have been proposed [7–13]. Some have tried to obtain fast computation of Zernike moments by allowing a loss of accuracy. Mukundan [7] has proposed a square-to-circular transform that treats rectangular images as circular ones. Gu [8] has proposed an iterative method based on the square-to-circular transform. However, the use of the square-to-circular transform always creates inaccurate sets of Zernike moments so that the reconstructed images have undesirable blocking effects. This means that the Zernike moments obtained by these methods are not suitable for systems that require accurate representation of images. Other approaches for fast computation of Zernike moments have tried to remove the redundancy in computing the radial polynomials. Because the factorial terms in the radial polynomials take most of the computation time to derive the Zernike moments, researchers have tried to remove the factorials by introducing a recurrence relationship. Prata [9] and Kintner [10] have both introduced their own recurrence relation to the Zernike radial polynomials, respectively. Belkasim [11] also proposed an algorithm that uses the radial and

* Corresponding author. Tel.: +82 2 2220 0561.
E-mail address: sunkyoo@vision.hanyang.ac.kr (S.K. Hwang).

0031-3203/$30.00
doi:10.1016/j.patcog.2006.03.004

angular expansions of Zernike orthogonal polynomials for fast computation of Zernike moments. Recently, Chong [12] proposed the q-recursive method which uses the recurrence relation of radial polynomials of fixed order n and varying repetition m. He also proposed a modified Kintner's method which is applicable in cases when the order, n, and the repetition, m, have the following relationship: $n = m$ and $n - m = 2$. Among the methods proposed by Belkasim, Kintner and Prata, the q-recursive method and the modified Kintner's method show the best performance. A slightly improved hybrid method that combines a simplified Kintner's method and other existing methods has been proposed by Wee [13]. Even though these fast methods successfully reduced the computational complexity when computing a series of Zernike moments by using the recurrence relation of the Zernike radial polynomials, the results showed some limitations. Even if only a single Zernike moment is needed, these methods require the computation of extra Zernike moments because these methods use the recurrence relation of the radial polynomials. In addition, these methods fail to focus on the computational complexity for the generation of Zernike basis functions and the projection of the image onto the basis functions.

In this paper, we present a novel approach to the fast computation of Zernike moments, which focuses on the reduction of the computational complexity of Zernike basis functions. As the Zernike basis functions have specific symmetric or anti-symmetric properties about the x-axis, the y-axis, the origin, and the straight line $y = x$, we can obtain the Zernike moments from an input image by computing only an octant of the Zernike basis functions. As a result, the proposed method computes the Zernike moments eight times faster than conventional methods. The proposed method can be applicable either to the computation of the full set or just the subset of Zernike moments. When computing a series of Zernike moments, the proposed method can be used with other fast methods for computing Zernike radial polynomials such as Kintner's or Chong's method, and such a mixed method shows the best performance on computation time.

This paper also presents an accurate form of Zernike moments for discrete image functions, which has been reported incorrectly in previous research. When computing Zernike moments from a discrete image, the normalization term is dependent upon the number of pixels involved in the computation. We present the exact form of discrete Zernike moments in Section 2 and show the correctness of the form in the experiments.

The outline of this paper is as follows: The next section describes Zernike moments in detail including their discrete form. In Section 3, existing fast methods for computing Zernike moments are described. Section 4 details the proposed method for computing Zernike moments by introducing the symmetric or anti-symmetric properties of the Zernike basis functions. Experimental results are given in Section 5 and the conclusions follow in Section 6.

2. Zernike moments

The computation of Zernike moments from an input image consists of three steps: computation of radial polynomials, computation of Zernike basis functions, and computation of Zernike moments by projecting the image on to the basis functions. In this section, we describe each procedure for the computation of Zernike moments in detail and present the exact form of Zernike moments for a discrete image function.

The procedure for obtaining Zernike moments from an input image begins with the computation of Zernike radial polynomials. The real-valued 1-D radial polynomial $R_{nm}(\rho)$ is defined as

$$R_{nm}(\rho) = \sum_{s=0}^{(n-|m|)/2} c(n, m, s)\rho^{n-2s}, \tag{1}$$

where

$$c(n, m, s) = (-1)^s \frac{(n-s)!}{s!((n+|m|)/2-s)!((n-|m|)/2-s)!}.$$

In (1), n and m are generally called order and repetition, respectively. The order n is a non-negative integer, and the repetition m is an integer satisfying $n - |m| = (\text{even})$ and $|m| \leqslant n$. The radial polynomials satisfy the orthogonal properties for the same repetition,

$$\int_0^{2\pi}\int_0^1 R_{nm}(\rho, \theta)R_{n'm}(\rho, \theta)\rho \,\mathrm{d}\rho \,\mathrm{d}\theta = \begin{cases} \dfrac{1}{2(n+1)} & \text{if } n = n', \\ 0 & \text{otherwise.} \end{cases} \tag{2}$$

Fig. 1shows the radial polynomials through order 5 in the interval $0 \leqslant \rho \leqslant 1$ for the low values of m.

Using the radial polynomial, complex-valued 2-D Zernike basis functions, which are defined within a unit circle, are formed by

$$V_{nm}(\rho, \theta) = R_{nm}(\rho)\exp(jm\theta), \quad |\rho| \leqslant 1, \tag{3}$$

where $j = \sqrt{-1}$. Zernike basis functions are orthogonal and satisfy

$$\int_0^{2\pi}\int_0^1 V_{nm}^*(\rho, \theta)V_{pq}(\rho, \theta)\rho \,\mathrm{d}\rho \,\mathrm{d}\theta = \begin{cases} \dfrac{\pi}{n+1} & \text{if } n = p,\ m = q, \\ 0 & \text{otherwise.} \end{cases} \tag{4}$$

The orthogonality implies no redundancy or overlap of information between the moments with different orders and repetitions. This property enables the contribution of each moment to be unique and independent of the information in an image.

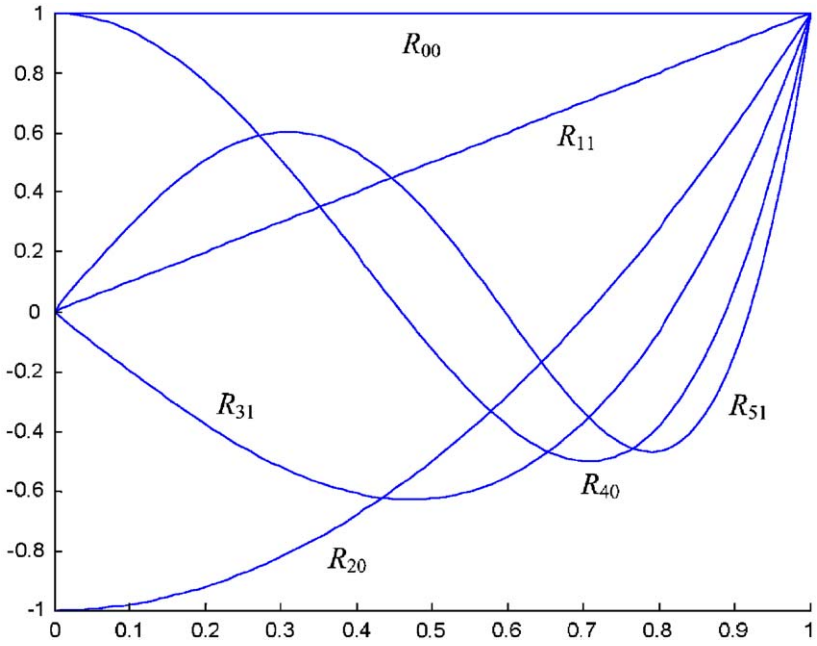

Fig. 1. Zernike radial polynomials of order 0–5 with low repetitions.

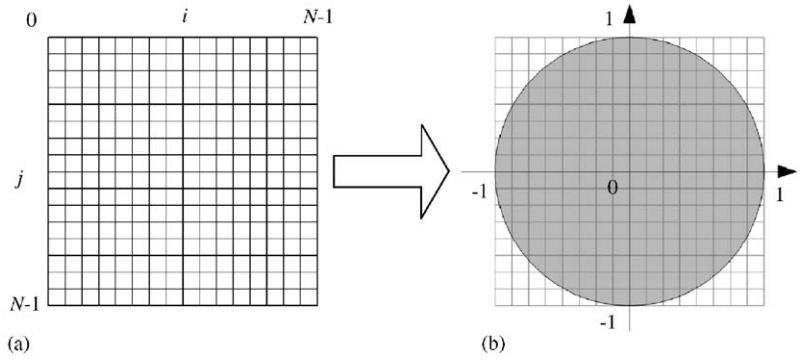

Fig. 2. General case of mapping transforms for normalization.

Complex Zernike moments of order n with repetition m are finally defined as

$$Z_{nm} = \frac{n+1}{\pi} \int_0^{2\pi} \int_0^1 f(\rho, \theta) V_{nm}^*(\rho, \theta) \rho \, \mathrm{d}\rho \, \mathrm{d}\theta, \tag{5}$$

where $f(x, y)$ is the image function and $*$ denotes the complex conjugate. As can be seen from the definition, the procedure for computing Zernike moments can be seen as an inner product between the image function and the Zernike basis function.

To compute Zernike moments from a digital image, the integrals in (5) are replaced by summations and the coordinates of the image must be normalized into [0, 1] by a mapping transform. Fig. 2 illustrates a general case of the mapping transform. In this case, the pixels located on the outside of the circle are not involved in the computation of the Zernike moments. Accordingly, Zernike moments computed by the mapping transform do not describe the properties of the outside of the unit circle in the image. The discrete form of the Zernike moments of an image size $N \times N$ is expressed as follows:

$$\begin{aligned} Z_{nm} &= \frac{n+1}{\lambda_N} \sum_{x=0}^{N-1} \sum_{y=0}^{N-1} f(x, y) V_{nm}^*(x, y) \\ &= \frac{n+1}{\lambda_N} \sum_{x=0}^{N-1} \sum_{y=0}^{N-1} f(x, y) R_{nm}(\rho_{xy}) \exp(-jm\theta_{xy}), \end{aligned} \tag{6}$$

where $0 \leqslant \rho_{xy} \leqslant 1$ and λ_N is a normalization factor. In some previous research, λ_N has been neglected or reported incorrectly [1,12]. In the discrete implementation of Zernike moments, the normalization factor λ_N must be the number of pixels located in the unit circle by the mapping transform, which corresponds to the area of a unit circle π in the

FUNCTION RadialPolynomial(ρ, n, m)
radial = 0
for s = 0 to (n–m)/2

$$c = (-1)^s \frac{(n-s)!}{s!\left(\frac{n+|m|}{2}-s\right)!\left(\frac{n-|m|}{2}-s\right)!}$$

$$radial = radial + c * \rho^{n-2s}$$

end for
return *radial*

FUNCTION ZernikeMoments(n, m)
$z_r = 0$
$z_i = 0$
cnt = 0
for y = 0 to N–1
  for x = 0 to N–1

$$\rho = \frac{\sqrt{(2x-N+1)^2+(N-1-2y)^2}}{N}$$

    if $\rho \le 1$
      radial = RadialPolynomial(ρ, n, m);

$$theta = \tan^{-1}\left(\frac{N-1-2y}{2x-N+1}\right)$$

      $z_r = z_r + f(x, y)$ * *radial* * cos(m*$theta$)
      $z_i = z_i + f(x, y)$ * *radial* * sin(m*$theta$)
      cnt = *cnt* + 1
    end if
  end for
end for

return $\frac{n+1}{cnt}(z_r + jz_i)$

Fig. 3. Pseudocode for computing Zernike moments.

continuous domain. We show the validity of the presented form of the normalization factor λ_N by the experiments in Section 5. The transformed distance ρ_{xy} and the phase θ_{xy} at the pixel of (x, y) are given by

$$\rho_{xy} = \frac{\sqrt{(2x-N+1)^2+(N-1-2y)^2}}{N},$$
$$\theta_{xy} = \tan^{-1}\left(\frac{N-1-2y}{2x-N+1}\right). \quad (7)$$

Fig. 3 shows the pseudocode for computing Zernike moments of order n with repetition m by Eq. (6). In Fig. 3, the real and imaginary parts of the Zernike moment are denoted by z_r and z_i, respectively. We assume the image size is $N \times N$.

3. Existing fast methods

As the computation of Zernike 1-D radial polynomials contains many factorial terms, most of the time taken for the computation of Zernike moments is due to the computation of radial polynomials. Therefore, researchers have proposed faster methods that reduce the factorial terms by utilizing the recurrence relations on the radial polynomials.

Prata [9] proposed a recurrence relation among $R_{nm}(\rho)$, $R_{(n-1)(m-1)}(\rho)$ and $R_{(n-2)m}(\rho)$ as follows:

$$R_{nm}(\rho) = \frac{2\rho n}{n+m} R_{(n-1)(m-1)}(\rho) + \frac{n-m}{n+m} R_{(n-2)m}(\rho). \quad (8)$$

Kintner [10] proposed another relation as shown below:

$$R_{nm}(\rho) = \frac{(K_2\rho^2 + K_3)R_{(n-2)m}(\rho) + K_4 R_{(n-4)m}(\rho)}{K_1}, \quad (9)$$

where the coefficients K_1, K_2, K_3 and K_4 are defined as

$$K_1 = \frac{(n+m)(n-m)(n-2)}{2},$$
$$K_2 = 2n(n-1)(n-2),$$
$$K_3 = -m^2(n-1) - n(n-1)(n-2),$$
$$K_4 = -\frac{n(n+m-2)(n-m-2)}{2}.$$

As can be seen from Eq. (9), Kintner used polynomials of varying low-order n with a fixed repetition m to compute the

radial polynomials. Therefore, Kintner's method is useful when Zernike moments with selected repetitions are needed as pattern features. When using Kintner's method, Zernike moments with $n=m$ or $n-m=2$ are computed directly by the definitions.

Recently, Chong presented the q-recursive method, which uses a relation of the radial polynomials of fixed order n and varying repetition m [12]. Because Chong denoted the repetition term as q instead of m, it is called the q-recursive method. The relation of the radial polynomial is defined as

$$R_{nm}(\rho)=H_1 R_{n(m+4)}(\rho)+\left(H_2+\frac{H_3}{\rho^2}\right) R_{n(m+2)}(\rho), \tag{10}$$

where

$$H_1=\frac{(m+4)(m+3)}{2}-(m+4)H_2 + \frac{H_3(n+m+6)(n-m-4)}{8},$$

$$H_2=\frac{H_3(n+m+4)(n-m-2)}{4(m+3)}+(m+2),$$

$$H_3=-\frac{4(m+2)(m+1)}{(n+m+2)(n-m)}.$$

As the order is fixed in Eq. (10), the individual order of Zernike moments can be calculated independently without referring to higher or lower order moments. Chong also proposed two relations when $n=m$ or $n-m=2$, which are denoted as the modified Kintner's method:

$$\begin{cases} R_{nn}(\rho)=\rho^n & \text{if } n=m, \\ R_{n(n-2)}(\rho)=n\rho^n-(n-1)\rho^{n-2} & \text{if } n-m=2. \end{cases} \tag{11}$$

From the experiments in [12], the combined use of both the q-recursive method and modified Kintner's method takes the shortest time to compute a full set of Zernike moments followed by Kintner's method. Especially, Chong's method is much faster than other methods in computing Zernike moments with a fixed order, which makes Chong's method more effective in cases where only selected orders of Zernike moments are used as feature vectors.

However, these methods have some limitations. Even if only a single Zernike moment is required, these methods require the computation of extra Zernike moments because they use recurrence relations. For example, when computing a single Zernike moment of $Z_{4,0}$ by using Chong's method, extra Zernike moments with higher repetitions such as $Z_{4,4}$ and $Z_{4,2}$ need to be additionally computed. Moreover, these methods focus only on the computation of Zernike radial polynomials and do not contribute to the reduction of computational complexity for the generation of Zernike basis functions or aid in obtaining Zernike moments by projection of the basis functions onto the image functions.

4. Novel approach to fast computation of Zernike moments

In this section, we describe a novel approach to the fast computation of Zernike moments by using the symmetric or anti-symmetric properties of the basis functions. In fact, the symmetric or anti-symmetric properties are first introduced in the computation of angular radial transform [14]. The properties described in this section are very similar but with further extension of [14]. As a result, the proposed method significantly reduces the number of pixels involved in the computation of Zernike moments. This method can also be used with existing fast methods for computing Zernike radial polynomials such as Kintner's or Chong's method, as will be demonstrated in the experiment.

4.1. Symmetry or anti-symmetry of Zernike basis functions

When there is a point $\mathbf{P}(a,b)$ on Cartesian coordinates, the symmetrical points with respect to the x-axis, the y-axis, the origin, and the line $y=x$ can be easily obtained. The coordinates of these symmetrical points are calculated simply by adding a negative sign to a or b, or swapping a and b. The Euclidean distance from the origin to these symmetrical points is the same. If θ is the phase of the point $\mathbf{P}(a,b)$, the phase of the symmetrical points can be expressed in terms of θ and π. Table 1 shows the properties of the symmetrical points.

Now let us investigate the definition of Zernike basis functions again. Because the Zernike basis functions $V_{nm}(x,y)$ are defined in the complex domain, using Euler's formula, one can write the equation as

$$V_{nm}(x,y)=VR_{nm}(x,y)+jVI_{nm}(x,y), \tag{12}$$

$$\begin{cases} VR_{nm}(x,y)=R_{nm}(\rho)\cos(m\theta), \\ VI_{nm}(x,y)=R_{nm}(\rho)\sin(m\theta), \end{cases}$$

where $VR_{nm}(x,y)$ and $VI_{nm}(x,y)$ are the real and imaginary parts of $V_{nm}(x,y)$, respectively.

The values of $R_{nm}(\rho)$ at the symmetrical points in Table 1 are identical to each other because they have the same value of ρ. Therefore, the value of the Zernike basis functions on these symmetrical points differs only by $\cos(m\theta)$ and $\sin(m\theta)$. As the sinusoidal function is a periodic function with a regular waveform, $VR_{nm}(x,y)$ and $VI_{nm}(x,y)$ have specific symmetric or anti-symmetric

Table 1
Properties of the symmetrical points of $\mathbf{P}(a,b)$

Axis of symmetry	Coordinates	Distance	Phase
$y=x$	$\mathbf{Q}_1(b,a)$	ρ	$\frac{\pi}{2}-\theta$
y-axis	$\mathbf{Q}_2(-a,b)$	ρ	$\pi-\theta$
The origin	$\mathbf{Q}_3(-a,-b)$	ρ	$\pi+\theta$
x-axis	$\mathbf{Q}_4(a,-b)$	ρ	$-\theta$

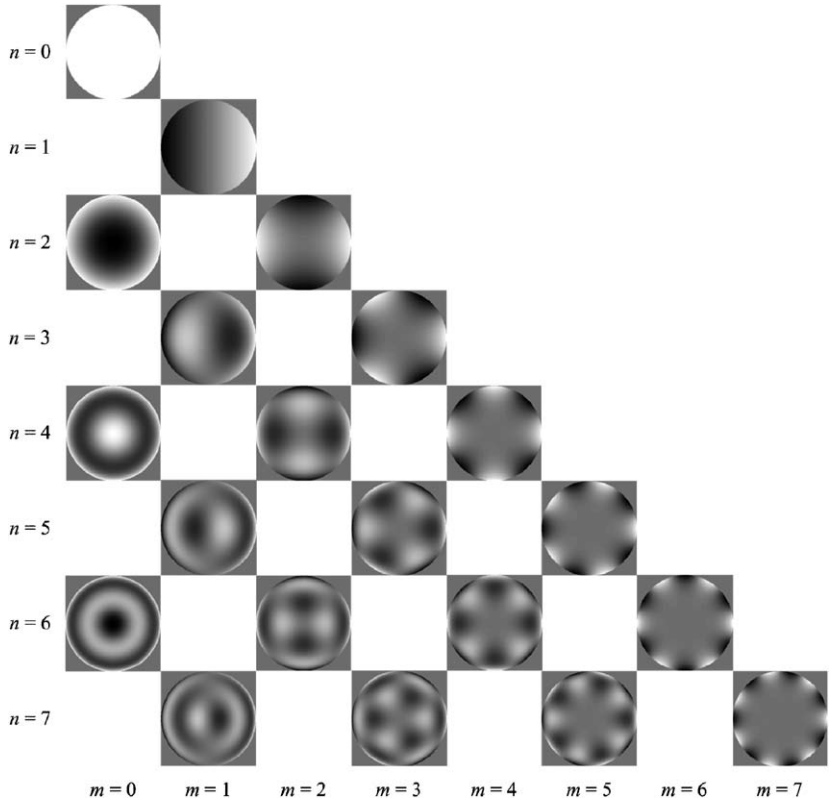

Fig. 4. Real parts of Zernike basis functions.

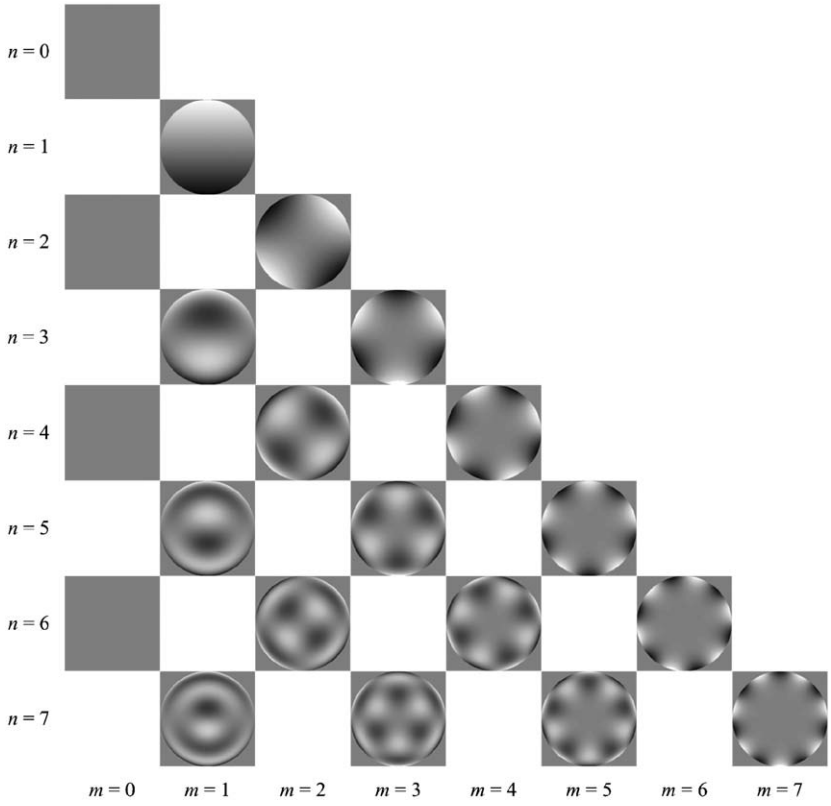

Fig. 5. Imaginary parts of Zernike basis functions.

properties. These symmetric or anti-symmetric properties generally depend on the value of the repetition.

The real and imaginary parts of the 2-D Zernike basis functions are drawn as grayscale images in Figs. 4 and 5, respectively. Each image is generated by mapping the range of the values of the Zernike basis functions ([−1, 1]) to the grayscale range ([0, 255]) linearly. The spatial coordinates $\{(x, y)\}$ are also normalized to a unit circle centered at the origin. The outer region of the unit circle is set to zero. The symmetry or anti-symmetry about the x-axis, the y-axis, and the origin can be easily found. For example, the real part of the Zernike basis functions with $n = m = 1$ is symmetric about the x-axis and anti-symmetric about the y-axis. Other basis functions have their own symmetry or anti-symmetry as the repetition changes.

In order to create equations that represent the symmetry and anti-symmetry of the Zernike basis functions, we suppose that there is a point **P** in the first quadrant. The points $\mathbf{Q}_n$ $(n = 1, 2, 3, 4)$ are the symmetrical points of **P**, which are summarized in Table 1. The values of the Zernike basis functions at the symmetrical points can then be obtained by adding a negative sign or not to the value of the Zernike basis functions at **P**. Here, the symmetrical relation is classified by the value of the repetition. When the repetition is an even number, that is $m = 2k$ $(k = 0, 1, 2, \ldots)$, the relationship is written as

$$\begin{aligned}
&VR_{n,2k}(\mathbf{Q}_2) = VR_{n,2k}(\mathbf{P}), \quad VI_{n,2k}(\mathbf{Q}_2) = -VI_{n,2k}(\mathbf{P}),\\
&VR_{n,2k}(\mathbf{Q}_3) = VR_{n,2k}(\mathbf{P}), \quad VI_{n,2k}(\mathbf{Q}_3) = VI_{n,2k}(\mathbf{P}),\\
&VR_{n,2k}(\mathbf{Q}_4) = VR_{n,2k}(\mathbf{P}), \quad VI_{n,2k}(\mathbf{Q}_4) = -VI_{n,2k}(\mathbf{P}). \quad (13)
\end{aligned}$$

When the repetition is an odd number, $m = 2k + 1$ $(k = 0, 1, 2, \ldots)$, the relationship is written as

$$\begin{aligned}
&VR_{n,2k+1}(\mathbf{Q}_2) = -VR_{n,2k+1}(\mathbf{P}),\\
&VI_{n,2k+1}(\mathbf{Q}_2) = VI_{n,2k+1}(\mathbf{P}),\\
&VR_{n,2k+1}(\mathbf{Q}_3) = -VR_{n,2k+1}(\mathbf{P}),\\
&VI_{n,2k+1}(\mathbf{Q}_3) = -VI_{n,2k+1}(\mathbf{P}),\\
&VR_{n,2k+1}(\mathbf{Q}_4) = VR_{n,2k+1}(\mathbf{P}),\\
&VI_{n,2k+1}(\mathbf{Q}_4) = -VI_{n,2k+1}(\mathbf{P}). \quad (14)
\end{aligned}$$

For the symmetrical point with respect to the line $y = x$, the symmetric or anti-symmetric properties can be grouped in four cases as follows:

$$\begin{aligned}
&VR_{n,4k}(\mathbf{Q}_1) = VR_{n,4k}(\mathbf{P}),\\
&VI_{n,4k}(\mathbf{Q}_1) = -VI_{n,4k}(\mathbf{P}),\\
&VR_{n,4k+1}(\mathbf{Q}_1) = VI_{n,4k+1}(\mathbf{P}),\\
&VI_{n,4k+1}(\mathbf{Q}_1) = VR_{n,4k+1}(\mathbf{P}),\\
&VR_{n,4k+2}(\mathbf{Q}_1) = -VR_{n,4k+2}(\mathbf{P}),\\
&VI_{n,4k+2}(\mathbf{Q}_1) = VI_{n,4k+2}(\mathbf{P}),\\
&VR_{n,4k+3}(\mathbf{Q}_1) = -VI_{n,4k+3}(\mathbf{P}),\\
&VI_{n,4k+3}(\mathbf{Q}_1) = -VR_{n,4k+3}(\mathbf{P}). \quad (15)
\end{aligned}$$

Note that, when the repetition is an odd number, the real and imaginary parts of the Zernike basis functions at the point $\mathbf{Q}_1$ refer to its imaginary and real part at point **P**.

To make it easy to understand the symmetric or anti-symmetric properties of the Zernike basis functions clearly, we briefly summarize the properties in Fig. 6. Only the first octant colored gray in each circle of Fig. 6 is the region that is actually computed. The values of the Zernike basis functions in the other white regions are obtained by flipping the value of that in the first octant. For example, in Fig. 6(a), the first octants labeled $\mathbf{R_0}$ and $\mathbf{S_0}$ are the real regions to be computed by the definition of the Zernike basis functions. The values of the Zernike basis functions in the other regions are obtained by flipping the value of the basis functions in the gray regions with respect to the line $y = x$, the y-axis, and the x-axis. If there is a minus sign, then the values are multiplied by -1 after they are flipped. If the repetition m is an even number, the real and imaginary parts of the Zernike basis functions only refer to their first octant, respectively. However, if the repetition m is an odd number, the real parts of Zernike basis functions refer to the first octant of both the real and imaginary parts of the Zernike basis functions. In short, once an octant of either the real or imaginary part of the Zernike basis functions is computed, the remaining regions of the unit circle can be simply obtained by flipping them because the Zernike basis functions have either symmetric or anti-symmetric properties.

4.2. Proposed method for fast computation of Zernike moments

The procedure for computing Zernike moments from an input image is essentially the same as projecting the input image onto the Zernike basis functions. In conventional methods, all pixels within the unit circle have to be multiplied by the value of the Zernike basis functions at the same location. In the proposed method, however, the Zernike moments can be obtained with an octant of the basis functions by using the symmetric or anti-symmetric properties of the basis functions. By using these properties, we can reduce some computational complexity for projecting the input image onto the Zernike basis functions by eliminating much of the multiplication operations.

Eq. (5) can be rewritten in complex form:

$$\begin{aligned}
Z_{nm} &= \frac{n+1}{\pi} \int\int_{x^2+y^2 \leqslant 1} f(x, y)[VR_{nm}(x, y)\\
&\quad - jVI_{nm}(x, y)]\,\mathrm{d}x\,\mathrm{d}y\\
&= \frac{n+1}{\pi} \int\int_{x^2+y^2 \leqslant 1} R_{nm}(\rho)\\
&\quad \times [f(x, y)\cos(m\theta) - jf(x, y)\sin(m\theta)]\,\mathrm{d}x\,\mathrm{d}y. \quad (16)
\end{aligned}$$

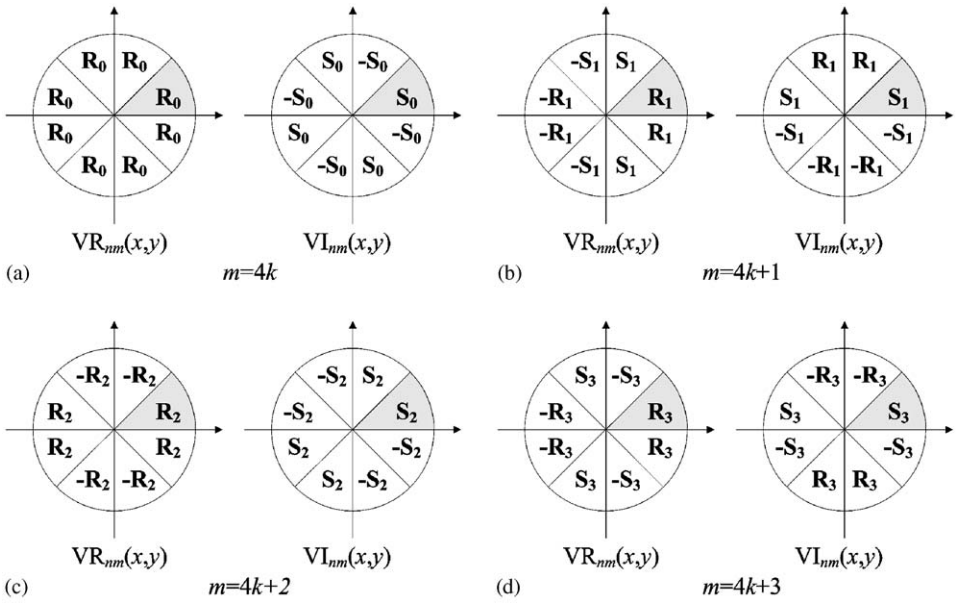

Fig. 6. Brief diagram of the symmetric or anti-symmetric properties of Zernike basis functions.

Both $VR_{nm}(x, y)$ and $VI_{nm}(x, y)$ have their specific symmetry or anti-symmetry as the repetition changes. Therefore, by using these properties as denoted in Fig. 6, we can rewrite the above equation with a new notation $g^r_m(x, y)$ and $g^i_m(x, y)$:

$$Z_{nm} = \frac{n+1}{\pi} \int\int_{\substack{x^2+y^2 \leqslant 1 \\ 0 \leqslant x \leqslant 1, 0 \leqslant y \leqslant x}} R_{nm}(\rho) \times [g^r_m(x, y) - j g^i_m(x, y)] \, dx \, dy. \quad (17)$$

In Eq. (17), $g^r_m(x, y)$ and $g^i_m(x, y)$ are computed by using the values of the image function and the sinusoidal functions at eight points in Fig. 7, and are related to the real and imaginary parts of the Zernike moments, respectively. Note that the integral range is only an octant of a unit circle as denoted in gray in Fig. 7. We can group $g^r_m(x, y)$ and $g^i_m(x, y)$ into four cases:

where h_i $(i = 1, 2, \ldots, 8)$ is the value of the image function at point $\mathbf{P}_i$ in Fig. 7 and the coordinates of the point $\mathbf{P}_1$ in the first octant are (x, y). As can be seen in Eqs. (17) and (18), the total number of multiplications necessary is reduced to about one-fifth while the number of additions remains the same, which contributes to a slight improvement in computation time.

Because the proposed method focuses only on the computation of Zernike basis functions and Zernike moments, existing fast methods such as Kintner's or Chong's method can be used in the computation of radial polynomials. If a set of Zernike moments with a fixed order is required, Chong's method is desirable. If a set of Zernike moments with a fixed repetition is required, Kintner's method is better. We provide a quantitative analysis of the computation time in the next section.

$$\begin{aligned}
g^r_{4k}(x, y) &= [h_1 + h_2 + h_3 + h_4 + h_5 + h_6 + h_7 + h_8] \cos(m\theta), \\
g^i_{4k}(x, y) &= [h_1 - h_2 + h_3 - h_4 + h_5 - h_6 + h_7 - h_8] \sin(m\theta), \\
g^r_{4k+1}(x, y) &= [h_1 - h_4 - h_5 + h_8] \cos(m\theta) + [h_2 - h_3 - h_6 + h_7] \sin(m\theta), \\
g^i_{4k+1}(x, y) &= [h_1 + h_4 - h_5 - h_8] \sin(m\theta) \quad + [h_2 + h_3 - h_6 - h_7] \cos(m\theta), \\
g^r_{4k+2}(x, y) &= [h_1 - h_2 - h_3 + h_4 + h_5 - h_6 - h_7 + h_8] \cos(m\theta), \\
g^i_{4k+2}(x, y) &= [h_1 + h_2 - h_3 - h_4 + h_5 + h_6 - h_7 - h_8] \sin(m\theta), \\
g^r_{4k+3}(x, y) &= [h_1 - h_4 - h_5 + h_8] \cos(m\theta) + [-h_2 + h_3 + h_6 - h_7] \sin(m\theta), \\
g^i_{4k+3}(x, y) &= [h_1 + h_4 - h_5 - h_8] \sin(m\theta) + [-h_2 - h_3 + h_6 + h_7] \cos(m\theta), \quad (18)
\end{aligned}$$

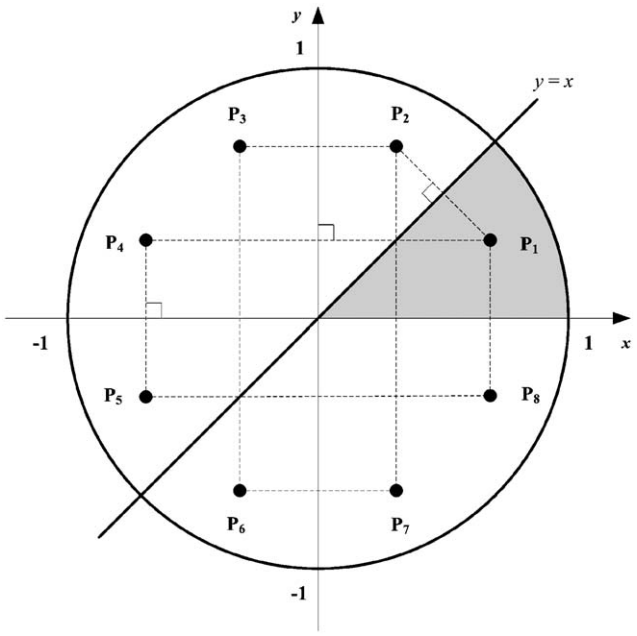

Fig. 7. Notations for eight symmetrical points.

5. Experimental results

5.1. Computation of discrete Zernike moments

To illustrate how well formula (6) approximates (5) we consider the computation of some of the Zernike moments for a simple image function using both formulae, and compared the results. A simple image function, $I(x, y)$, is selected

$$I(x, y) = \begin{cases} 1 & \text{if } y \geqslant 0, \\ 0 & \text{if } y < 0, \end{cases} \tag{19}$$

where $x^2 + y^2 \leqslant 1$. The full set of Zernike moments with order 0 to 4 is computed from the image. When using Eq. (5), we computed the Zernike moments mathematically. When using Eq. (6), we generated a 512×512 discrete image as shown in Fig. 8 and computed the Zernike moments using a program implemented with Microsoft^{TM} visual C++ 6.0. The computed Zernike moments using each method are reported in Table 2. The explicit form of the radial polynomials in Table 2 is referred from [15].

Note that the two sets of Zernike moments are almost the same. The errors found at the fourth decimal place can be seen as quantization errors. From the experiment we confirmed that the discrete form of Zernike moments in Eq. (6) is valid.

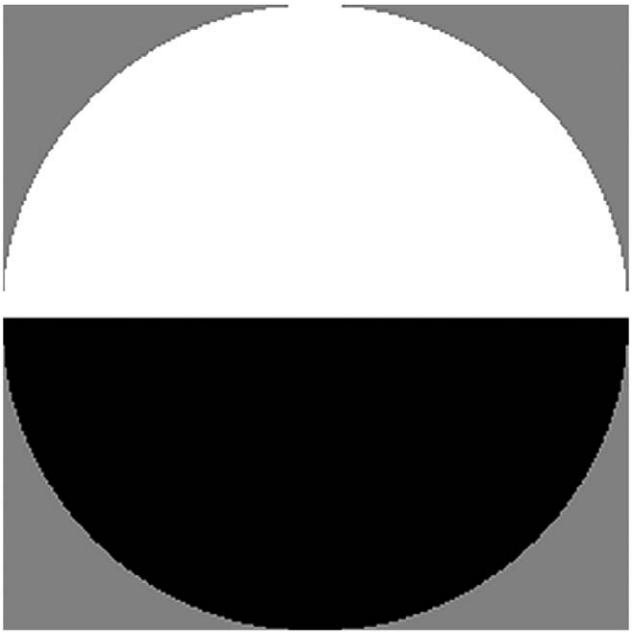

Fig. 8. Test image for the computation of discrete Zernike moments.

Table 2
Comparison of Zernike moments computed in continuous and discrete domains

Zernike moments	Radial polynomials	By Eq. (5)	By Eq. (6)
Z_{00}	1	0.5	$0.500000 + j0.000000$
Z_{11}	ρ	$-j0.42441$	$0.000000 - j0.424407$
Z_{20}	$2\rho^2 - 1$	0	$0.000033 + j0.000000$
Z_{22}	ρ^2	0	$0.000000 + j0.000000$
Z_{31}	$3\rho^3 - 2\rho$	j 0.169765	$0.000000 + j0.169758$
Z_{33}	ρ^3	$-j0.169765$	$0.000000 - j0.169640$
Z_{40}	$6\rho^4 - 6\rho^2 + 1$	0	$0.000055 + j0.000000$
Z_{42}	$4\rho^4 - 3\rho^2$	0	$0.000000 + j0.000000$
Z_{44}	ρ^4	0	$0.000265 + j0.000000$

Fig. 9. Test image for the comparison of computation time.

Table 3
CPU elapsed time for computing Zernike moments

Maximum order	Computation time (ms)					
	Direct	Kintner's	q-recursive	Proposed	Kintner' s + proposed	q-recursive + proposed
12	2473	1749	1783	462	240	244
24	15415	6844	7161	1983	920	995
36	44438	14772	14814	5639	1892	2096
48	145822	26026	27003	18581	3562	3893

Table 4
CPU elapsed time for computing Zernike moments with a specific order

Selected order	Computation time (ms)					
	Direct	Kintner's	q-recursive	Proposed	Kintner' s + proposed	q-recursive + proposed
12	441	982	296	66	137	45
24	2270	6143	897	299	826	131
36	5005	7665	794	627	977	115
48	10102	13359	1327	1283	1865	166

Table 5
CPU elapsed time for computing Zernike moments with a specific repetition

Selected repetition	Computation time (ms)					
	Direct	Kintner's	q-recursive	Proposed	Kintner' s + proposed	q-recursive + proposed
0	6215	855	12887	798	124	1869
2	5997	1126	11755	782	180	1623
4	5744	873	11150	747	123	1505
6	4916	324	3505	641	52	541
9	4352	206	2368	563	40	422

5.2. Fast computation of Zernike moments

To examine the computation time more explicitly, a number of experiments were completed. In the first experiment, we computed the full set of Zernike moments with different maximum orders using methods which included the direct method, the q-recursive method, Kintner's method, the proposed method, and finally mixed methods that combine the proposed method with q-recursive and Kintner's method, respectively. The direct method denotes the computation of Zernike moments using the definitions, that is, Eq. (6). The modified Kintner's method is used together in the implementation of the q-recursive and Kintner's method. The maximum order was set to 12, 24, 36, and 48. If the maximum order was 12 then 49 Zernike moments from $Z_{0,0}$ to $Z_{12,12}$ are computed by each method. As a test image, a 256×256 grayscale image shown in Fig. 9 is used. The experiment was performed with a 1.7 GHz Pentium IV PC with 512Mbyte RAM and was implemented with Microsoft^{TM} visual C++ 6.0. The CPU elapsed times for each method are tabulated in Table 3. From the results, the combined methods listed in the last two columns take less time in general than the other methods in computing the full set of Zernike moments. We confirmed that all the values of the Zernike moments generated by each method are the same.

In the second experiment, the time for computing Zernike moments is measured for the selected order of 12, 24, 36, and 48. For example, if the selected order was 12 then we computed the Zernike moments of $Z_{12,0}, Z_{12,2}, \ldots, Z_{12,12}$. The experimental results are shown in Table 4. The mixed method with q-recursive and the proposed method show the best performance in this case.

The computation was also done for the individual repetition of Zernike moments. The selected repetitions were 0, 2, 4, 6, and 9. We set the maximum order to 48, so that if the selected repetition is 9, $Z_{48,9}$, $Z_{48,18}$, $Z_{48,27}$, $Z_{48,36}$, and $Z_{48,45}$ are computed. The CPU elapsed times for computing Zernike moments with selected repetitions are reported in Table 5. The mixed method with Kintner's method and the proposed method shows the best performance in this case.

In the last experiment, we measured the computation time for computing a single Zernike moment. We selected $Z_{6,2}$, $Z_{12,0}$, $Z_{25,13}$, and $Z_{44,20}$ randomly and computed these moments by each method. The computation time by each

Table 6
CPU elapsed time for computing a single Zernike moment

Individual Zernike moment	Computation time (ms)					
	Direct	Kintner's	q-recursive	Proposed	Kintner' s + proposed	q-recursive + proposed
$Z_{6,2}$	225	443	465	26	59	88
$Z_{12,0}$	282	336	371	30	47	76
$Z_{25,13}$	408	160	184	46	77	95
$Z_{44,20}$	760	845	1066	97	116	163

Table 7
Recommended methods for computing Zernike moments

Feature	Recommended method
When a single Zernike moment is required	Proposed method
When the entire set of Zernike moments is required	Proposed method + q-recursive method *or* Proposed method + Kintner' s method
When the entire set of Zernike moments with an individual order is required	Proposed method + q-recursive method
When the entire set Zernike moments with individual repetition is required	Proposed method + Kintner' s method

method is reported in Table 6. In this case, the proposed method shows the best performance among these methods. As the q-recursive and Kintner's method cannot compute an individual Zernike moment, these methods must compute extra Zernike moments to use the recurrence relation and take more time than even the direct method.

From the experiments above, we confirmed that the proposed method reduces the time needed for computing Zernike moments to about one-eighth of existing methods. Here, we summarize the recommended method for computing Zernike moments in Table 7 case by case. When a single Zernike moment is required, the use of the proposed method is recommended. When computing a set of Zernike moments, the mixed method, which combines the proposed method and q-recursive or Kintner's method, gives the best performance. Note that the proposed method reduces the computation time in every case.

6. Conclusion

In this paper we proposed a fast and accurate method for computing Zernike moments from a digital image. The method utilizes the symmetric or anti-symmetric properties of Zernike basis functions. With the proposed method, only an octant of the basis functions is required to compute the Zernike moments, which means that the number of pixels involved in the computation of Zernike moments is only one-eighth of existing methods. The proposed method can be used with either the computation of a single Zernike moment or a set of Zernike moments. When computing a set of Zernike moments, the proposed method can be used with other existing fast methods such as Kintner's or the q-recursive method, and this mixed method shows the best performance. From the experimental results, we confirm that the proposed method successfully reduces the computation time in every case.

References

[1] A. Khotanzad, Y.H. Hong, Invariant image recognition by Zernike moments, IEEE Trans. Pattern Anal. Mach. Intell. 12 (5) (1990) 489–497.

[2] M.R. Teague, Image analysis via the general theory of moments, J. Opt. Soc. Amer. 70 (1980) 920–930.

[3] W.Y. Kim, P. Yuan, A practical pattern recognition system for translation, scale and rotation invariance, Proceedings of IEEE International Conference on Computer Vision and Pattern Recognition, June 1994, pp. 391–396.

[4] Y.S. Kim, W.Y. Kim, Content-based trademark retrieval system using visually salient feature, J. Image Vision Comput. 16 (1998) 931–939.

[5] L. Wang, G. Healey, Using Zernike moments for the illumination and geometry invariant classification of multispectral texture, IEEE Trans. Image Process. 7 (2) (1998) 196–203.

[6] W.Y. Kim, Y.S. Kim, Robust rotation angle estimator, IEEE Trans. Pattern Anal. Mach. Intell. 21 (8) (1999) 768–773.

[7] R. Mukundan, K.R. Ramakrishnan, Fast computation of Legendre and Zernike moments, Pattern Recognition 28 (9) (1995) 1433–1442.

[8] J. Gu, H.Z. Shu, C. Toumoulin, L.M. Luo, A novel algorithm for fast computation of Zernike moments, Pattern Recognition 35 (12) (2002) 2905–2911.

[9] A. Prata, W.V.T. Rusche, Algorithm for computation of Zernike polynomials expansion coefficients, Appl. Opt. 28 (1989) 749–754.

[10] E.C. Kintner, On the mathematical properties of the Zernike polynomials, Opt. Acta. 23 (8) (1976) 679–680.

[11] S.O. Belkasim, Efficient algorithm for fast computation of Zernike moments, IEEE 39th Midwest Symposium on Circuits and Systems, vol. 3, 1996, pp. 1401–1404.

[12] C.W. Chong, P. Raveendran, R. Mukundan, A comparative analysis of algorithms for fast computation of Zernike moments, Pattern Recognition 36 (3) (2003) 731–742.

[13] C.Y. Wee, R. Paramesran, F. Takeda, New computational methods for full and subset Zernike moments, Inform. Sci. 159 (3–4) (2004) 203–220.

[14] S.K. Hwang, W.Y. Kim, A fast and efficient method for computing ART, IEEE Trans. Image Process. 15 (1) (2006).

[15] S.M. Abdallah, E.M. Nebot, D.C. Rye, Object recognition and orientation via Zernike moments, Proceedings of Asian Conference on Computer Vision, January 1998, pp. 386–393.

About the Author—S.K. HWANG received the B.S. and M.S. degreee in electronic engineering from Hanyang University, Seoul, Korea in 1997 and 1999, respectively. Currently, he is pursuing the Ph.D. degree in electronic engineering at Hanyang University. His research interests include shape representation, motion segmentation, and pattern recognition.

About the Author—W.Y. KIM received the B.S. degree in electronic engineering from Hanyang University, Seoul, Korea in 1980. He received the M.S. degree from Pennsylvania State University, University Park, in 1983 and the Ph.D. degree from Purdue University, Sest Lafayatte in 1989, both in electrical engineering. From 1989 to 1994, he was with Erik Jonsson School of Engineering & Computer Science, University of Texas at Dallas. Since 1994, he has been on the faculty of Electrical & Computer Engineering at Hanyang University. His research interests inculde visual surveillance, face tracking and identificatin, motion analysis, face recognition, and MPEG-7 applications where he contributed to the development of MPEG-7 visual descriptors.